JOURNAL OF MATERIALS SCIENCE 8 (1973) 467–474

Precipitation (exsolution) in an orthopyroxene

P. E. CHAMPNESS, G. W. LORIMER
Department of Geology and Department of Metallurgy, Faculty of Science, University of Manchester, UK

Ion-thinned samples of orthopyroxene from the Stillwater complex, Montana, have been examined in the electron microscope at 100 and 1000 kV. Exsolution lamellae of a calcium-rich, monoclinic pyroxene (augite) up to 0.5 μm in width were observed parallel to (100) of the matrix. The interface between the matrix and precipitate is semi-coherent and consists of a regular network of dislocations. Nucleation occurs at grain boundaries, subgrain boundaries and individual dislocations. Subsequent growth takes place by the movement of ledges along the (100) interface.

The matrix orthopyroxene also contains coherent, homogeneously-distributed precipitates (GP zones). A precipitate-free zone occurs adjacent to each augite lamella.

1. Introduction

X-ray diffraction investigations coupled with optical microscopy have been successful in identifying the products formed during phase transformations in many silicate minerals. However, until the development of ion-thinning techniques [1-4] coupled with the use of the high-resolution tool of transmission electron microscopy very little was known about the *mechanism* of phase transformations in silicates. Transmission electron microscopic studies of the alkali and plagioclase feldspars [5-8] and of clinopyroxenes [4, 9] have shown that the microstructures produced during exsolution* are consistent with the decomposition of the parent phase by the mechanism of spinodal decomposition. (The spinodal mechanism does not require nucleation but involves the growth of sinusoidal composition waves with progressively increasing wavelength and amplitude [10].)

In the present paper evidence is presented for the decomposition of orthopyroxene† by a phase transformation mechanism involving both nucleation and growth. Heterogeneous nucleation sites have been identified and evidence is also presented for the homogeneous nucleation of a calcium-rich phase.

The orthopyroxene is a bronzite‡ with composition approximately $Mg_{0.81}Fe_{0.16}Ca_{0.03}SiO_3$ from the Stillwater complex, Montana [11] which exhibits a lamellar structure parallel to (100) in the optical microscope. Henry [12] examined a number of orthopyroxenes from plutonic rocks which exhibited lamellar structures and came to the conclusion that the lamellae had the same composition as the matrix and were formed by deformation. Hess [11] found that the misorientation between lamellae could be seen optically and was entirely in the orthopyroxene host. He concluded that, because the lamellae had a higher birefringence than the matrix, they were an exsolved Ca-rich monoclinic pyroxene (augite§), but that there was too small a volume fraction to produce reflections on single crystal X-ray photographs.

Boyd and Brown [13] examined a Stillwater bronzite in an electron probe microanalyser and attributed variations in the Ca$K\alpha$ scan to the exsolution of a calcium-rich phase. Although the resolution of the microprobe was not sufficient

*Phase separation from a solid solution is called "exsolution" by mineralogists.
†Pyroxenes are single-chain silicates of Mg, Fe and Ca with the general formula $MSiO_3$. Mg-rich, Ca-poor varieties are orthorhombic, Pbca, with $a \sim 18.3$, $b \sim 8.9$, $c \sim 5.2$ Å.
‡Bronzites contain from 10 to 30 mol % $FeSiO_3$.
§"Augite" contains more than 25 mol % $CaSiO_3$ and "subcalcic augite" from 15 to 25 mol % $CaSiO_3$. Subcalcic augite is a metastable phase.

for separate quantitative analyses of either the matrix or the exsolved phase to be made, Boyd and Brown estimated that the lamellae were 1 to 2 μm thick and that the volume fraction was too large for them to have an augite composition; therefore they must be subcalcic augite§.

2. Experimental

Samples for electron microscopy were prepared from conventional uncovered petrographic thin sections using the techniques described by Barber [1] and Champness and Lorimer [4] which enables a direct correlation to be made between the light-optical and electron-optical microstructures. Each sample was thinned in an Edwards IBMA1 ion-thinning machine until perforation occurred. Preliminary examination of the samples was carried out in a conventional electron microscope operating at 100 kV. Selected specimens were then examined in an A.E.I. EM 7 electron microscope operating at 1000 kV. The penetration of the electron beam is approximately a linear function of voltage for light elements and thus the use of the high-voltage electron microscope enables the observation of areas of the specimen several microns thick, as compared to the few thousand of ångströms transparent to electrons at 100 kV. The extra penetration was particularly valuable when determining the distribution of phases and in correlating the structure observed in the electron microscope with that observed optically.

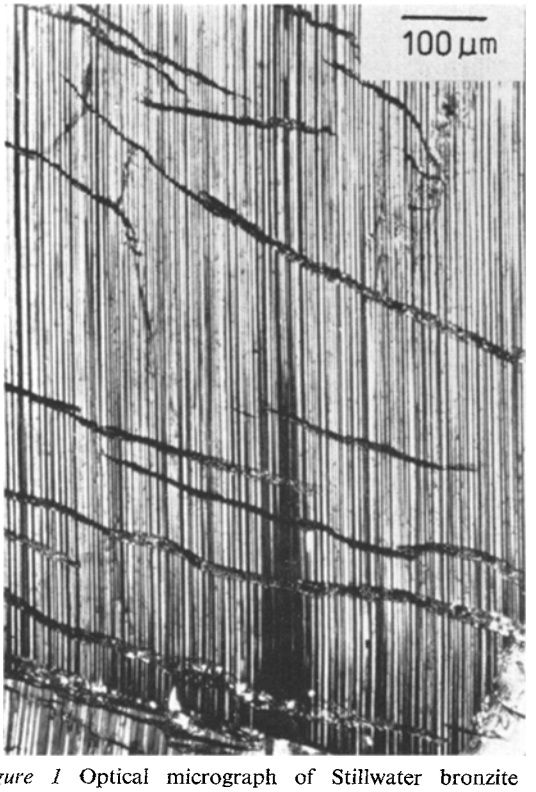

Figure 1 Optical micrograph of Stillwater bronzite (crossed polars) showing lamellar structure parallel to (100). Electron micrographs in Figs. 2 and 3 are from this area.

Figure 2 Low-magnification transmission electron-micrograph (1000 kV) of grain in Fig. 1. The electron beam is approximately parallel to (100). The volume fraction of lamellae is obviously much lower than it appears to be in Fig. 1.

3. Precipitate morphology and distribution

3.1. Optical and electron microscopy

The predominant feature seen in the optical microscope is the lamellae which are parallel to (100) (Fig. 1). On the electron-optical scale the distribution of the phases can be seen more clearly as shown in the series of micrographs, Figs. 2-4, taken at progressively higher magnifications. (Figs. 1-3 are all micrographs of the same pyroxene grain.) In Fig. 2 long, thin lamellae, approximately 0.1 μm thick can be seen running

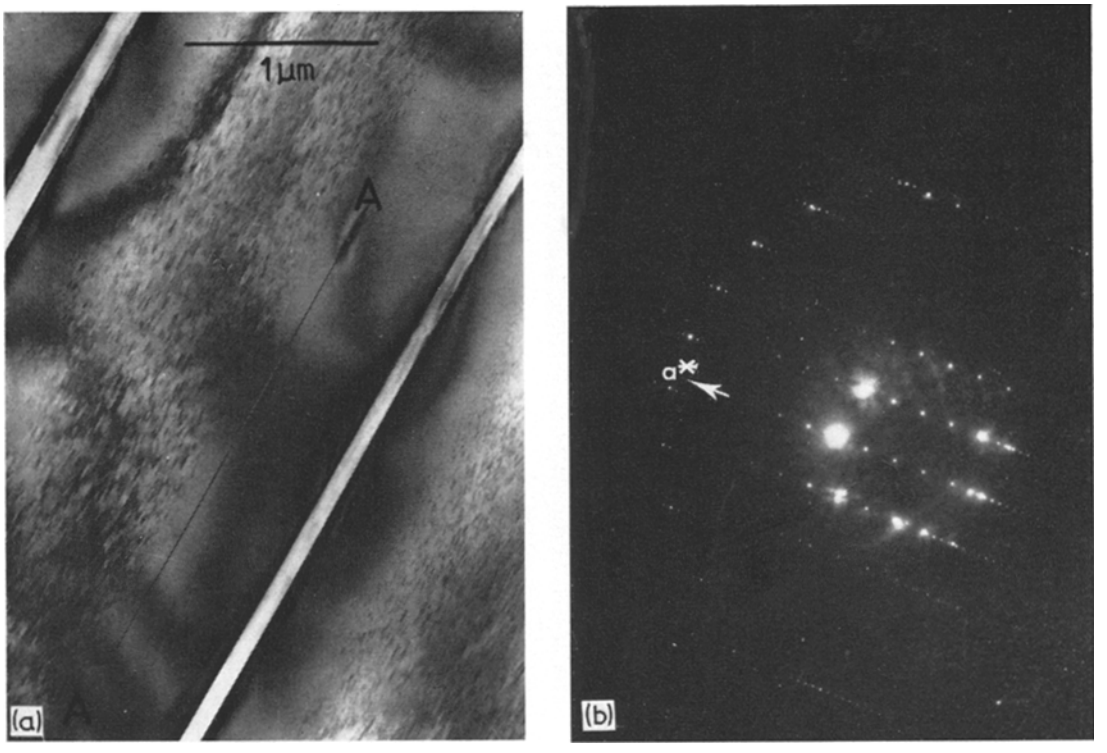

Figure 3 (a) Electron micrograph (100 kV) showing details of precipitate distribution. Two large augite lamellae are visible together with one thin lamella (AA) and a fine, homogeneous distribution of GP zones. Precipitate-free zones occur adjacent to both types of augite lamella. (b) Diffraction pattern taken with selected-area aperture centred over one of the large augite lamellae. The centre of the pattern is produced solely by the augite while reflections from both the augite and the matrix ortho-pyroxene occur in the periphery of the first Laue zone and in the second Laue zone.

across the field of view parallel to (100)*. In Fig. 3a the lamellae show a complex contrast at their boundary with the matrix which is due to the strain fields associated with structural defects (ledges) as discussed below. In the region between these lamellae a second set of thin (100) lamellae, often only about 18Å thick, are present and may extend for several microns. An estimate of the volume fraction of the lamellar precipitates made from low-magnification, high-voltage micrographs similar to that shown in Fig. 2 gave a value of 1.4%, a figure much lower than might be estimated from the optical micrograph in Fig. 1.

Diffraction patterns of the lamellae (Fig. 3b) indicate that they have the structure of diopside, a monoclinic pyroxene with space group C2/c and $a \sim 9.7$, $b \sim 8.9$, $c \sim 5.3$Å, $\beta \sim 106°$. Suitably oriented foils, such as that in Fig. 4, show that the interface between each lamella and the matrix orthopyroxene is semi-coherent and is composed of a regular array of misfit dislocations.

In the areas between the lamellae there is a fine homogeneously-distributed phase (Fig. 5). The precipitates are coherent plates (Fig. 5b) which form on (100) of the matrix, are approximately 0.2 μm in diameter and only one matrix lattice-parameter thick [15]. Their structure is different from that of the large lamellae (they are not imaged under the same diffraction conditions) and their size is a function of the distance from the clinopyroxene precipitates. They gradually decrease in size as a large lamella is approached and a PFZ (precipitate-free-zone) occurs immediately adjacent to each lamella (Figs. 3a and 7).

Despite the marked misorientation which can be seen in optical thin sections of the Stillwater

*The bumpy surface of the sample is a product of the specimen preparation technique [14], and the dark contour running across the lamellae is a diffraction effect (extinction contour) and should not be confused with structural detail

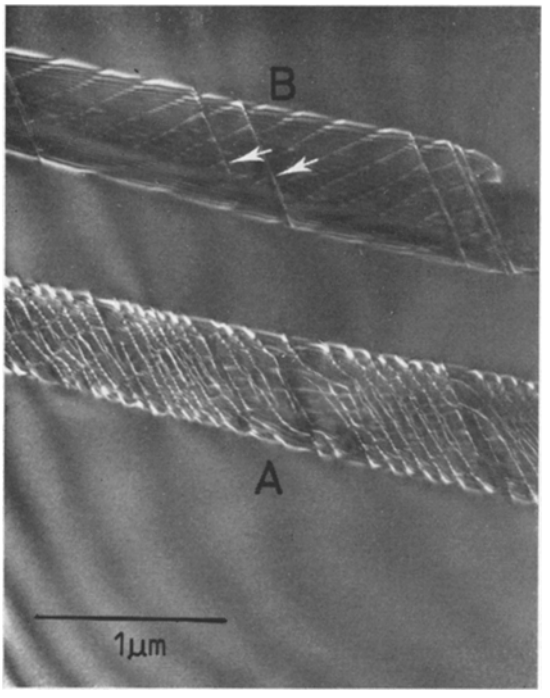

Figure 4 Dark-field electron micrograph (100 kV) taken using weak-beam technique and showing interfacial dislocations on lamella A and growth ledges (arrowed) on lamella B. Electron beam approximately parallel to [100].

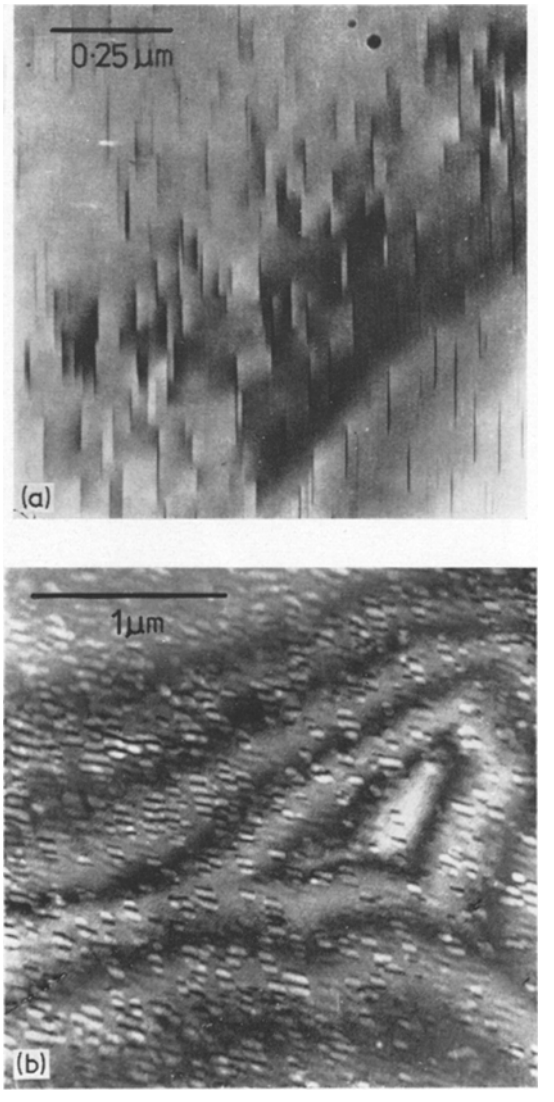

Figure 5 (a) Bright-field electron micrograph (100 kV) of GP zones showing extensive strain contrast in the matrix. The zones are one matrix lattice-parameter thick and lie on (100). Electron beam parallel to (100). (b) Dark-field electron micrograph (100 kV) of GP zones where the electron beam is approximately parallel to [100]. Zones exhibit displacement-fringe contrast and are fully coherent with the matrix.

bronzite and which can be detected by single-crystal X-ray diffraction [11], no features attributable to deformation, apart from the very occasional subgrain boundary (Fig. 7), were detected. We therefore conclude that the misorientation is a result of strain-fields at the semi-coherent inter-phase boundaries which extend a considerable way into the matrix.

3.2. Analytical electron microscopy

Lorimer and Champness [16] used the analytical electron microscope EMMA-4 to monitor the variation in calcium between two of the lamellae and to determine the concentration of calcium in the exsolved clinopyroxene. The analytical procedure and the technique by which a quantitative analysis was made is given in detail by these authors; for the present discussion it is sufficient to state that a chemical analysis can be carried out in EMMA-4 by forming a probe 0.1 to 0.2 μm in diameter and detecting simultaneously on separate spectrometers, the characteristic X-ray intensities for two elements in the sample. This ratio is, under most circumstances in thin foils, independent of the specimen thickness and can be used to monitor variations in chemical composition [16-18].

Fig. 6 illustrates diagrammatically the distribution of calcium which Lorimer and Champness found between two of the large calcium-rich

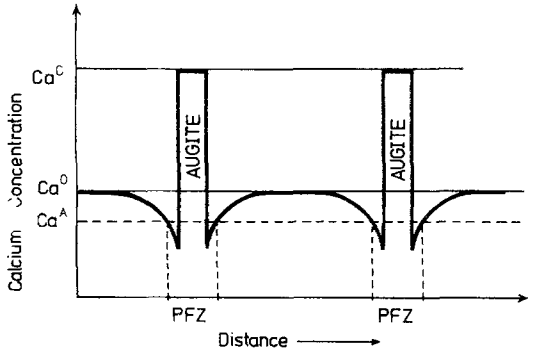

Figure 6 Schematic illustration of variation in calcium concentration between two lamellae. Ca° is the initial calcium concentration in the matrix, Ca^{c} is the concentration in the augite lamellae and Ca^{A} is the critical calcium concentration for the nucleation and/or growth of the GP zones. The extent of the precipitate free zones is indicated.

lamellae. The calcium content immediately adjacent to the lamellae is lower than that at a point mid-way between the lamellae.

By using external thin-foil standards of known calcium and silicon content, the large clinopyroxene lamellae were shown to contain 24 wt % CaO and thus have an augite, and not a subcalcic augite composition.

4. Precipitation mechanisms

4.1. The nucleation of the lamellae

Although the optical microstructure of the bronzite (Fig. 1) is similar to that of minerals which have exsolved by the mechanism of spinodal decomposition, the distribution of phases, when viewed on the electron-optical scale, is very different: rather than a modulated structure that is, at least in the early stages of the reaction, coherent with the matrix [5-9] the lamellae have a distinct interface with the matrix, even when they are only 18Å thick. As the diffraction evidence has shown (Fig. 3b) the structure of the large lamellae is different from that of the matrix. To form a precipitate which has a different structure (and composition) from the matrix it is necessary to produce a distinct interface between the precipitate and the matrix; the formation of this interface is synonymous with a nucleation event.

During slow cooling from a single-phase region heterogeneous nucleation at imperfections is preferred over homogeneous nucleation because of the reduction in strain energy which can be realized at these sites. During the present

Figure 7 Bright-field electron micrograph (100 kV) showing heterogeneous nucleation of augite on a subgrain boundary. The "organ-pipe" distribution has been produced by autocatalytic nucleation of successive lamellae.

investigation three heterogeneous nucleation sites have been identified: grain boundaries, subgrain boundaries and dislocations. The grain boundaries, being the most potent of the three sites, will have been the first structural defect at which nucleation occurred during cooling of the orthopyroxene and the lamellae will have grown without competition for solute from other modes of precipitation; it is thought that the thickest lamellae are those that were originally nucleated at grain boundaries.

Fig. 7 shows an example of the heterogeneous nucleation of the lamellae at a subgrain boundary. Although most of the lamellae are very thin, about 18Å, a few are several microns in length. Probably these were the first to nucleate and were able to grow without competition for solute. The amount of undercooling below the equilibrium solvus required to activate the nucleation sites on the subgrain boundary would have been greater than that for nucleation at grain boundaries, and thus these lamellae have not grown to nearly the same width as their precursors. Most

of the shorter lamellae which have nucleated at the sub-boundary are not randomly distributed but take the form of a row of "organ pipes". We propose that this distribution of precipitates arose by the autocatalytic nucleation of successive lamellae: the stress field associated with the growth of one lamella activated an adjacent, although as yet infertile, nucleation site in the subgrain boundary. This process was repeated and successive lamellae were nucleated, each being slightly shorter than that nucleated immediately previously because it has had a slightly shorter time in which to grow.

The third heterogeneous nucleation site is dislocations within the grains. A nucleation event is shown in Fig. 8 where the unit dislocation has split into two partial dislocations to form a layer of precipitate one matrix lattice-parameter thick. The original dislocation was probably formed on the (100) of the matrix (the normal slip plane [19]) as a result of stresses produced during cooling. The splitting of the unit dislocations into partials may have occurred during stress-induced motion on the (100) planes or may have followed the segregation of calcium to the original dislocation. The process of segregation of solute to a unit dislocation followed by the splitting of the dislocation into partials to nucleate a second phase occurs during the formation of γ' precipitates in aluminium-silver alloys where a dislocation reaction of the type

$$\tfrac{1}{2}[\bar{1}10] \rightarrow \tfrac{1}{6}[\bar{1}2\bar{1}] + \tfrac{1}{6}[\bar{2}11]$$

produces a layer of the precipitate one lattice parameter thick on the (111) matrix plane [20]. Nucleation of the α_2 phase in titanium-aluminium alloys also occurs by a similar mechanism [21] where a precipitate of the α_2 phase one lattice parameter thick is produced by a dislocation reaction of the type

$$\tfrac{1}{3}[110] \rightarrow \tfrac{1}{3}[100] + \tfrac{1}{3}[010].$$

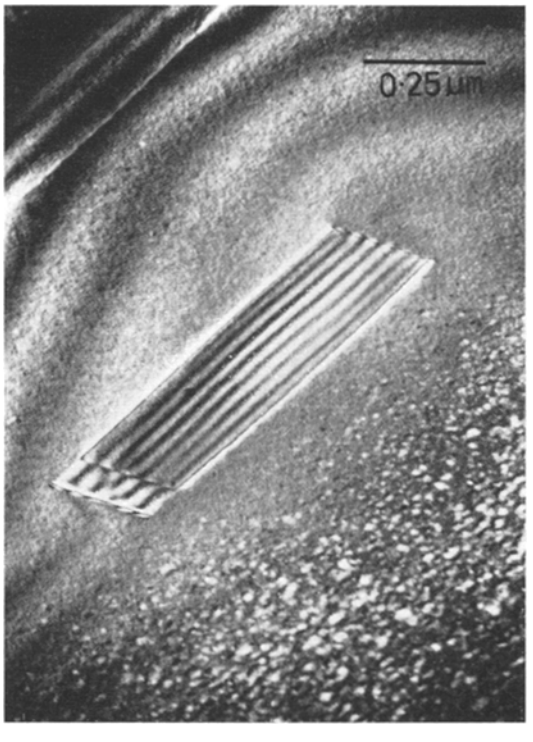

Figure 8 Dark-field electron micrograph (100 kV) showing nucleation of augite lamellae by the formation of a stacking fault on (100). (g = 002.)

4.2. Growth of the lamellae

Following nucleation, the growth of the lamellae along the (100) matrix plane can occur rapidly by the propagation of a partial dislocation along the (100) plane. Diffusion is faster in this plane than perpendicular to it as shown by the asymmetry of the PFZs around the lamellae in Figs. 3 and 7 and will favour the formation of a thin augite lamella. Growth of the lamellae perpendicular to the (100) face requires both the nucleation of another layer of augite on the surface of the first thin precipitate and the diffusion of solute, mainly calcium, to the interface. The calcium-concentration profile formed adjacent to lamellae, shown schematically in Fig. 6 [16] is evidence that the diffusion of solute to the lamellae may have been the rate-controlling step in the growth of, at least, the thinner lamellae. The complex contrast effects observed at the lamella/matrix interface in Fig. 3 are strain fields produced by the ledges on the (100) face of the augite lamella which can be seen in the (100) foil of Fig. 4. It is proposed that the growth of the lamellae perpendicular to (100) occurs by the propagation of these ledges, which vary in height from one to several lattice parameters [15].

The growth of precipitates by the migration of ledges across the matrix/precipitate interface is a well-documented phenomenon in the metallurgical literature and detailed observations have been made of the motion of ledges during growth of γ' plates in aluminium-silver [22], κ plates in copper-silicon [23] and grain boundary precipitates in various steels [24].

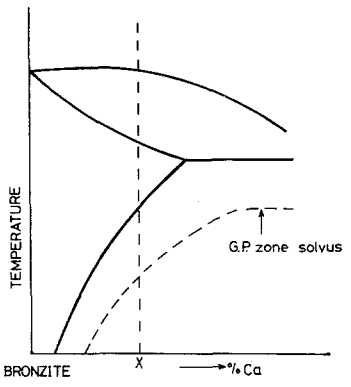

Figure 9 Schematic representation of stable and metastable phase boundaries in pseudo-binary bronzite-augite system. Cooling of an orthopyroxene of composition X results in heterogeneous nucleation of augite at a temperature just below the equilibrium solvus (solid line) while GP zones form when the temperature has fallen below the GP zone solvus. See text for discussion.

4.3. The formation of the coherent precipitates

The fine, coherent precipitates between the lamellae in Figs. 3, 5 and 7 have lattice parameters which are different from those of the matrix, as there is considerable strain in the matrix around the particles (Fig. 5a). They are calcium-rich, as evidenced by the PFZ adjacent to the lamellae, where the EMMA-4 results show that the calcium concentration is low [16]. Metastable precipitates with a similar structure to, but a different composition from the matrix are known as GP (Guinier-Preston) zones* in metal alloys, and it is proposed that the fine homogeneously distributed precipitates in the orthopyroxenes are calcium-rich GP zones.

GP zones form as a metastable or "transition" phase in many alloys; their crystallography and morphology is particularly well documented for alloys based on aluminium [27]. A metastable precipitate can form in preference to the equilibrium phase if its crystal structure is more similar to the matrix than is that of equilibrium phase. This allows a "good fit" (coherency) between the matrix and the precipitate lattice in at least one direction, thus reducing the surface and strain energies required for the nucleation. The reduction in free energy will lead to an increase in the nucleation rate, at a given solute supersaturation, for the "transition" phase. In the orthopyroxene the GP zones are fully coherent with the matrix across their broad faces (Fig. 5), while the equilibrium precipitate, the augite, is only semi-coherent (Fig. 4), thus the criterion outlined above is satisfied. A schematic phase diagram in which the metastable GP-zone solvus has been included is shown in Fig. 9.

The coherent precipitates failed to nucleate in the PFZ because of the depletion of calcium in these regions. A critical concentration of calcium is necessary for the GP zones to nucleate and it is at this calcium concentration that the boundary of the PFZ† occurs. A schematic representation of the calcium distribution in the matrix and the position of the boundary of the PFZ is shown in Fig. 6. The GP zones at the edge of the PFZ are smaller than those in the regions distant from the lamellae (Fig. 3a and 7) because the growth of the zones was restricted due to depletion of calcium.

5. Conclusions

The precipitation (exsolution) of the calcium-rich phase in the orthopyroxene studied occurs by mechanisms involving both nucleation and growth. Heterogeneous nucleation of augite occurs at grain boundaries, subgrain boundaries and dislocations. Growth involves migration of ledges across the (100) faces of the precipitates.

Homogeneous nucleation of GP zones occurs subsequently in the region of the matrix between the lamellae. A PFZ is formed adjacent to the lamellae as a result of calcium depletion.

Acknowledgements

The authors would like to thank Professors R. B. Nicholson, E. Smith and J. Zussman for providing laboratory facilities. We are extremely grateful to Professor G. M. Brown for providing the sample of the Stillwater bronzite and to Mr J. Bradley for sample preparation. The high voltage electron microscopy was carried out at the BSC Swinden Laboratories, Rotherham. The 100 kV electron microscope and ion-thinning machines were provided by NERC.

References

1. D. J. BARBER, *J. Mater. Sci.* **5** (1970) 1.

*These are named after the co-discoverers (Guinier [25] and Preston [26]) of the precipitates in aluminium-copper alloys.
†PFZs have been observed in a number of aluminium alloys [27] and their origin in an aluminium-zinc-magnesium alloy has been discussed in detail by Unwin *et al* [28].

2. A. H. HEUER, R. F. FIRESTONE, J. D. SNOW, H. W. GREEN, R. G. HOWE, and J. M. CHRISTIE, *Rev. Sci. Instr.* **42** (1971) 1177.
3. P. GILLESPIE, A. C. MCLAREN, and J. N. BOLAND, *J. Mater. Sci.* **6** (1971) 87.
4. P. E. CHAMPNESS and G. W. LORIMER, *Contr. Mineral. Petrol.* **33** (1971) 17.
5. D. C. OWEN and J. D. C. MCCONNELL, *Nature Phys. Sci.* **230** (1971) 118.
6. *Idem*, Proceedings of NATO conference on the Feldspars, to be published.
7. H-U. NISSEN and W. BOLLMAN, Proc. IV Eur. Reg. Cong. Electron Microscopy (1968) 321.
8. M. KOREKAWA, H-U. NISSEN, and D. PHILIPP, *Z. Krist.* **131** (1970) 418.
9. P. E. CHAMPNESS and G. W. LORIMER, Proc. Vth Internat. Mat. Symp., Berkeley, California (California University Press, 1972) p. 1245.
10. H. I. AARONSON, G. W. LORIMER, P. E. CHAMPNESS, and E. T. C. SPOONER, in preparation.
11. H. H. HESS, *Geol. Soc. Amer. Mem.* **80** (1960).
12. N. F. M. HENRY, *Mineral. Mag.* **26** (1942) 179.
13. F. R. BOYD and G. M. BROWN, *Mineral. Soc. Amer. Spec. Pap.* **2** (1969) 211.
14. I. S. T. TSONG and D. J. BARBER, *J. Mater. Sci.* **7** (1972) 687.
15. P. E. CHAMPNESS and G. W. LORIMER, in preparation.
16. G. W. LORIMER and P. E. CHAMPNESS, *Amer. Mineral.*, in press.
17. G. W. LORIMER, M. J. NASIR, R. B. NICHOLSON, K. NUTTALL, D. E. WARD, and J. R. WEBB, Proc. Vth Internat. Mat. Symp., Berkeley, California (California University Press, 1972) p. 22.
18. G. CLIFF and G. W. LORIMER, Proc. V Eur. Cong. Electron Microscopy (1972) 140.
19. N. L. CARTER, *J. Geophys. Res.* **76** (1971) 5514.
20. R. B. NICHOLSON and J. NUTTING, *Acta Metallurgica* **9** (1961) 332.
21. M. J. BLACKBURN, "The Science, Technology and Application of Titanium" (Pergamon Press, Oxford, 1970) p. 633.
22. C. LAIRD and H. I. AARONSON, *Acta Metallurgica* **15** (1967) 73.
23. K. R. KINSMAN, H. I. AARONSON, and E. EICHEN, *Met. Trans.* **1** (1971) 1041.
24. K. R. KINSMAN and H. I. AARONSON in "Transformation and Hardenability in Steel" (Climax Molybdenum Co, Ann Arbor, Michigan, 1967) p. 39.
25. A. GUINIER, *Nature* **142** (1938) 569.
26. G. D. PRESTON, *ibid* **142** (1938) 570.
27. A. KELLY and R. B. NICHOLSON, *Prog. Mat. Sci.* **10** (1963) 151.
28. P. N. T. UNWIN, G. W. LORIMER, and R. B. NICHOLSON, *Acta Metallurgica* **17** (1969) 1363.

Received 20 September and accepted 26 October 1972.